REPORT DOCUMENTATION PAGE

Form Approved
OMB No. 0704-0188

1. AGENCY USE ONLY (Leave blank)	2. REPORT DATE	3. REPORT TYPE AND DATES COVERED
		FINAL REPORT

4. TITLE AND SUBTITLE
Stable High-Power Harmonic Gyro-Amplifiers

5. FUNDING NUMBERS
~~61102F~~
~~XXXXXX~~
62234N
0683/42

6. AUTHOR(S)
Prof Luhmann

7. PERFORMING ORGANIZATION NAME(S) AND ADDRESS(ES)
Univ of California, Los Angeles
Los Angeles, CA

8. PERFORMING ORGANIZATION REPORT NUMBER
AFOSR-TR-95-0327

9. SPONSORING/MONITORING AGENCY NAME(S) AND ADDRESS(ES)
AFOSR/NE
110 Duncan Avenue Suite B115
Bolling AFB DC 20332-0001

10. SPONSORING/MONITORING AGENCY REPORT NUMBER
AFOSR-91-0382

11. SUPPLEMENTARY NOTES

12a. DISTRIBUTION/AVAILABILITY STATEMENT
APPROVED FOR PUBLIC RELEASE: DISTRIBUTION UNLIMITED

12b. DISTRIBUTION CODE

13. ABSTRACT (Maximum 200 words)
SEE FINAL REPORT ABSTRACT

14. SUBJECT TERMS

15. NUMBER OF PAGES

16. PRICE CODE

17. SECURITY CLASSIFICATION OF REPORT	18. SECURITY CLASSIFICATION OF THIS PAGE	19. SECURITY CLASSIFICATION OF ABSTRACT	20. LIMITATION OF ABSTRACT
UNCLASSIFIED	UNCLASSIFIED	UNCLASSIFIED	UNCLASSIFIED

Stable High-Power Harmonic Gyro-Amplifiers

Final Report, 10/14/94

AFOSR Tri-Service Grant 91-0382

10/1/91 - 9/30/94

Principal Investigator: N. C. Luhmann, Jr.

Stable High-Power Harmonic Gyro-Amplifiers

Table of Contents

1. Bullet Summary

- 207 kW was generated by our second-harmonic smooth-bore gyro-TWT which was stable without rf input.
- Marginal Stability Design Procedure was developed for designing stable high-performance gyro-TWT amplifiers and verified by our second-harmonic gyro-TWT results.
- 1 MW stable output is predicted for our 140 GHz, third-harmonic smooth-bore gyro-TWT design.
- 70 kW slotted third-harmonic gyro-TWT was designed for Varian as their ARPA-funded 95 GHz fast-wave amplifier.
- High performance slotted third-harmonic gyro-TWT was tested by using axis-encircling electron beams produced by our gyroresonant rf accelerator and found to be stable.
- Third-harmonic 95 GHz, smooth-bore gyroklystron was designed capable of 70 kW output power with 20% efficiency, 30 dB gain and cw operation.
- Sixth-harmonic 95 GHz, slotted gyroklystron was designed capable of 84 kW output power with 12% efficiency and 27 dB gain.
- Broadband 0 dB input couplers were designed for the smooth-bore second-harmonic gyro-TWT and slotted third-harmonic gyro-TWT amplifiers with HP's finite-element HFSS electromagnetic design code.
- Broadband TE_{n1}/TE_{11} mode converters were developed for the high power overmoded output of the smooth-bore second-harmonic gyro-TWT and slotted third-harmonic gyro-TWT experiments.

2. Research Progress during 10/1/91--9/30/94

2.1 Summary

The focus of our Tri-Service University Research Program in Vacuum Electronics has been on basic research issues associated with operating harmonic gyrotron devices as high-power, coherent millimeter-wave amplifiers. Substantial theoretical and experimental progress has been achieved. We introduced the marginal stability design (MSD) procedure[1] for achieving stability in high-performance gyro-TWT's. We also concluded the initial tests of the high power, second-harmonic TE_{21} gyro-TWT amplifier which is based on the MSD procedure and the novel concept[1] that harmonic operation is capable of significantly increasing the output power because the start-oscillation beam current is much higher for the relatively weak harmonic interaction. **Indeed, the second-harmonic gyro-TWT amplifier's unprecedented output power of 207 kW exceeded the previous record-level of 120 kW, which was produced by a first-harmonic gyro-TWT. Our amplifier yielded an efficiency of 13%, a saturated gain of 16 dB with a bandwidth of 2% and was stable for zero rf input power.**

As another part of this grant's research, we designed a third-harmonic gyro-TWT amplifier for Varian as their 95 GHz fast-wave amplifier in their ARPA-funded development program. We tested lower frequency scaled models by using the axis-encircling electron beams produced by a gyroresonant rf accelerator. **A single-section amplifier verified the stability of the design and yielded a small-signal gain of 13 dB with 3% bandwidth. A two-section amplifier yielded a small-signal gain of 25 dB with 5% bandwidth,** but oscillated in a fourth-harmonic gyro-BWO mode due to an imperfect sever. The experiment will be continued and the nonlinear characteristics measured after the sever and coupler have been optimized.

We also extended the concept that harmonic gyro-TWT's can yield superior performance and designed a third-harmonic TE_{31} gyro-TWT that is predicted to generate an output power of 1 MW. In addition, we investigated high-harmonic gyroklystron amplifiers, which tend to be more stable than gyro-TWT's. We contributed to Litton's ARPA-funded slotted gyroklystron program by transferring our state-of-the-art self-consistent nonlinear slotted gyroklystron simulation code and also by publishing a paper describing the design of slotted harmonic gyroklystrons. A sixth-harmonic slotted gyroklystron was developed with a predicted output power of 84 kW, 12% efficiency and 27 dB gain. Of further importance for Litton, we found that a more robust smooth-bore circuit can yield equivalent parameters. A 70 kV smooth-bore third-harmonic gyroklystron was designed with a predicted output power of 70 kW with 20% efficiency, 35 dB gain and can even be operated cw with an acceptable level of wall heating.

Although we are actively working with Varian to use our slotted third-harmonic gyro-TWT design to develop a high-average-power, 95 GHz fast-wave amplifier for ARPA, the information on this work is also being actively disseminated to the microwave community to aid other companies and laboratories in the design of high power, high frequency fast-wave amplifiers. For example, we have offered to make available our rf accelerated electron beam source to test concepts developed by the various ARPA funded groups, including Northrop, NRL and Litton, in addition to Varian.

2.2 Gyro-TWT Marginal Stability Design Procedure

Although the gyro-TWT has long held considerable potential as a high power amplifier of millimeter-waves, good performance had eluded engineers for many years due to its tendency to oscillate[2] as a gyrotron. In collaboration with Drs. K.R. Chu and A.T. Lin, we developed the marginal stability design (MSD) procedure[1] for ensuring stability in a high performance gyro-TWT amplifier. The method utilizes linear analytical theory to determine the threshold for

instability. It first finds the maximum stable beam current for the chosen value of magnetic field and velocity ratio. The length of the interaction region is then chosen to be less than the shortest critical length for oscillation of all possible harmonic gyro-BWO[3] interactions. If the gain from this length of interaction is less than desired, then it can be increased by using several of these stable sections separated by attenuating severs[4] for isolation. A nonlinear simulation code should be used in order to evaluate the saturated performance. If the characteristics are not satisfactory, then one should iterate the steps with a new magnetic field and $v_\perp/v_\parallel$. We have used the MSD procedure to design the successful high power second-harmonic gyro-TWT and slotted third-harmonic gyro-TWT amplifiers that are discussed below in Secs. 2.3.1 and 2.4.2, respectively. This design procedure is likely to be employed in all future gyro-TWT designs.

2.3 High Power s^{th}-Harmonic TE_{s1} Gyro-TWT Amplifiers

The superb characteristics of this class of amplifier are due to three key features. The first is that there can be no competing first harmonic emission.[5] If a gyro-TWT is designed so that the electrons are in resonance at the s^{th}-harmonic with a cylindrical waveguide's TE_{s1} mode, then there are no modes which can be excited at the fundamental frequency, as can be seen in Fig. 1 for the case of a second-harmonic TE_{21} gyro-TWT. The second feature is that the allowable beam current for stability and therefore the output power is much higher[1,6] than at the fundamental frequency due to the weaker strength of the harmonic interactions, which leads to high power operation. Figure 2 shows that the critical beam current for the absolute instability in an s^{th}-harmonic TE_{s1} gyro-TWT increases strongly with the harmonic number. The third feature is that the required magnetic field can be reduced by a factor of s in a TE_{s1} gyro-TWT, which often allows conventional electromagnets or permanent magnets to be used for millimeter-wave generation rather than more troublesome superconducting systems.

2.3.1 Second-Harmonic TE_{21} Gyro-TWT

Utilizing an 80 kV, 20 A MIG beam with velocity ratio $v_\perp/v_\parallel = 1$, the second-harmonic TE_{21} gyro-TWT (Table I)[7,8] generated a record-high output power of 207 kW, corresponding to an efficiency of 13%. The measured saturated gain is 16 dB and the bandwidth is 2.1% as shown in Fig. 3. The transfer curve for the amplifier for several values of beam current shown in Fig. 4 displays the expected $I^{1/3}$ dependence of gain on current. The amplifier is stable for zero-drive power. The measured stability diagram is presented in Fig. 5 where the magnetic field for the onset of oscillation is normalized to the operating magnetic field. The stability of the single-stage amplifier is attributed to the well matched rf loads and input/output couplers that were designed with HP's HFSS electromagnetics design code. For another set of parameters, stable amplification could even be achieved with a gain as high as 38 dB, as shown in Fig. 6. Also, the cylindrical waveguide circuit had been sliced axially with two cuts though the axis and separated in azimuth by 90^o in order to destroy the competing TE_{31} gyro-BWO mode. Figure 7 shows the critical interaction length for oscillation of the strongest gyro-BWO interactions in the second-harmonic TE_{21} gyro-TWT amplifier. By destroying the odd-order azimuthal modes, the fourth-harmonic TE_{41} gyro-BWO becomes the most dangerous oscillation threat and the interaction section can thereby be roughly doubled. The round-trip attenuation of the unwanted TE_{11} mode was measured to be 52 dB, partially due to the teflon tube coated with lossy carbon that is inserted between the sliced circuit and vacuum jacket.

The proof-of-principle experiment was performed at 16 GHz. The circuit fits snugly inside a compact strong-back vacuum jacket and all vacuum seals are provided by Conflat flanges except for the two input and output microwave windows. The overmoded multi-hole, directional input coupler was measured to have an insertion loss of 1.4 dB over a bandwidth of 20% and a

selectivity of 98% into the desired TE_{21} mode. A second similar coupler with 3 dB coupling was built for monitoring the output wave. To ensure that all modes are terminated in the interaction waveguide, Carbon-coated MaCor tubes have been placed at both ends. Both terminations display an insertion loss of at least 20 dB with a minimum return loss of 15 dB. The output end also includes an electrically isolated Faraday Cup with an integral bending magnet to measure the transmitted electron beam.

The assembled device was positioned along the axis of a custom-designed aluminum foil-wound, water-cooled solenoid magnet which produces a 4 kG field with greater than 0.25% uniformity over 1 m and with a transverse field of less than 0.15%. Our single-anode MIG electron gun, which had been designed with the EGUN code at UCLA and then fabricated to our specifications by NTHU, was attached to the circuit and then evacuated to the 10^{-8} Torr range. The gun was pulsed to 100 kV by a 1.5 μs modulator.

2.3.2 Third-Harmonic TE_{31} Gyro-TWT

We have further extended the novel concept[1] that the relatively weak, harmonic gyrotron interactions give much higher values of threshold beam current for amplifier stability and thus can be utilized to generate extremely high power. We have designed a stable third-harmonic TE_{31} gyro-TWT[9] capable of generating power levels four times as high as achieved in our high-power, second-harmonic TE_{21} gyro-TWT. As had been shown in Fig. 2, the critical beam current for the absolute instability for a 100 kV axis-encircling beam with velocity ratio $v_\perp/v_\| = 1$ is increased from a fundamental-harmonic TE_{11} gyro-TWT by a factor of twenty-six for a third-harmonic TE_{31} gyro-TWT. In our marginal stability design procedure, a high-performance gyro-TWT is comprised of several interaction sections, each stable from the absolute instability in the operating mode and each shorter than the critical oscillation length for the strongest competing gyro-BWO mode, and isolated from neighboring sections by attenuating severs. An important feature of s^{th}-harmonic TE_{s1} gyro-TWT's with axis-encircling beams is that oscillation cannot occur[5] at harmonics lower than the operating harmonic. The critical length for oscillation of the dominant competing gyro-BWO modes in the third-harmonic gyro-TWT is shown in Fig. 8. Using this information, two separate megawatt-level, 140 GHz, 100 kV, 50 A, third-harmonic gyro-TWT's with $v_\perp/v_\| = 1$ and $\Delta v_\|/v_\| = 5\%$ have been designed[9] and are summarized in Table II. One device utilizes an axis-encircling electron beam and is predicted to generate 775 kW with 15.5% efficiency, 27 dB saturated gain, and a constant-drive bandwidth of 5% (see Fig. 9). The other device uses a more conventional MIG beam and is predicted to generate 940 kW with 18.7% efficiency, 30 dB saturated gain, and a constant-drive bandwidth of 5% .

2.4 Slotted High-Harmonic Gyro-TWT Amplifiers

Since axis-encircling electrons are in resonance with the s^{th}-order azimuthal mode of cylindrical waveguide when $\omega = s\Omega_c + k_\| v_\|$, high-harmonic gyrotron interaction offers the important advantage of a significantly reduced magnetic field requirement. To compensate for the weaker interaction, one can introduce an azimuthally corrugated interaction structure[10-12] which ripples the rf field lines in a way to strengthen a particular harmonic field component. The magnetron-like slotted structure is shown in Fig.10. The number of vanes, N, is chosen such that the strongest azimuthal field harmonic is equal to the desired cyclotron harmonic number s. As in the magnetron, the modes of interest are the 2π mode, where the phase in each slot is identical, and the π mode, where adjacent slots are out of phase by π. The π mode is more ideal for the harmonic gyro interaction because a high-order (N/2) azimuthal mode is dominant, whereas most of the energy of the 2π mode is wasted in the useless TE_{01} mode.

To design[13] a high gain slotted gyro-TWT, the inner vane radius a is chosen to be fairly close to the electron Larmor radius and the outer vane radius b is then chosen to obtain the correct cutoff frequency. To evaluate the slotted gyro-TWT, we wrote a nonlinear simulation code similar to that which Dr. Ganguly used for the slotted penio-TWT amplifier[12].

2.4.1 General Nonlinear Theory

An important difference between a harmonic gyrotron with an axis-encircling electron beam and a conventional gyrotron is that in the latter the beam bunches solely in gyro-phase space, while in the former the beam bunches azimuthally in real space as well as in gyro-phase space. The trajectories of the axis-encircling beam during a typical fourth-harmonic interaction are shown in Fig. 11. The initial unperturbed beam is shown in Fig. 11(a) and Fig.11(b) shows it early in the linear stage. The beam has begun to break into four sections corresponding to the four-fold symmetry of the TE_{41}-like mode. Figures 11(c) and 11(d) show the beam in the middle and late linear stage, respectively. The beam is azimuthally bunching into the four decelerating phases of the wave. Notice in Fig. 11(d) that phase-trapping is beginning to become evident. Figure 12 shows the predicted dependence of the slotted gyro-TWT's efficiency on the cyclotron harmonic number s. The efficiency, which is 42% at the second harmonic and drops to 10% at the eighth harmonic, seems to scale inversely with the harmonic number.

2.4.2 Third-Harmonic Slotted Gyro-TWT

We are actively working with Varian to develop[14,15] a high-average-power, 95 GHz fast-wave amplifier for ARPA. Our proof-of-principle scaled experiments are being performed at 10 GHz. Varian has accepted our design for a third-harmonic slotted gyro-TWT (Table III) which uses a 50 kV, 3 A, axis-encircling beam with $v_\perp/v_\parallel = 1.4$ and $\Delta v_\parallel/v_\parallel = 6\%$ The amplifief is predicted to produce 30 kW with 20% efficiency, 40 dB saturated gain and a 2.3% constant-drive bandwidth as shown in Fig. 13. The predicted spatial growth of power in the three-stage amplifier is shown in Fig. 14. Figure 15 shows that the operating mode is stable for the parameters of the system. By viewing the dispersion diagram in Fig. 16 for the slotted gyro-TWT, it can be seen that several harmonic gyro-BWO and penio-BWO modes can destabilize the amplifier. Figure 17 shows that oscillation in these modes can be suppressed for the design parameters.

The dual-feed overmoded multi-hole Miller-type[16], 0 dB directional input coupler shown in Fig. 18 was designed with the HP HFSS code. The HFSS predictions in Fig. 19 show that its bandwidth is ~20% and its selectivity into the π mode is excellent (~95%). It is predicted to be a good match for all modes in the interaction waveguide ($S_{33} \leq 0.2$). It was measured with our HP8510 Automated Vector Network Analyzer. It currently yields a coupling of ~10 dB with 20% bandwidth. Figure 20 shows that its selectivity into the desired π mode is ~90%.

For the high power output of this amplifier, the high-order wave will be transformed into the lowest order TE_{11} wave in a beat-wave mode converter.[17] Through our collaboration with Dr. Pretterebner of Dr. M. Thumm's electromagnetics simulation group, a broadband TE_{31} to TE_{11} mode converter (see Fig. 21) has been designed for our third-harmonic slotted gyro-TWT. Two TE_{31}/TE_{11} converter were fabricated and measured. As shown in Fig. 22, the four-period converter displays the desired 4% bandwidth with excellent converted mode purity (see Fig. 23).

Since the slotted gyro-TWT's Cusp[18-20] electron gun can not yet deliver an electron beam of sufficient quality, our gyroresonant rf accelerator[21] is employed to produce the requisite axis-encircling[22] electron beam. Our new accelerator cavity has successfully produced a 5 A, 70 kV axis-encircling electron beam with the acceleration characteristics shown in Fig. 24. The electron gun injector for the rf accelerator was a scaled-SLAC 5045 Klystron Pierce gun, which was

fabricated in-house. As mentioned above, we have offered to make this test-stand available to the various groups funded under ARPA's 95 GHz Fast-Wave Amplifier Initiative.

The slotted rf circuit for the proof-of-principle experiment was built using electric discharge wire machining. The circuit pieces bolt together and are aligned within an oversized vacuum chamber with knife-edge metal-seal Conflat flanges except for the two input and output microwave windows. The slotted third-harmonic gyro-TWT is being tested within a water-cooled copper solenoid which produces a 3 kG field with ±0.5% uniformity over 0.7 m. The discrete pancake magnets allow the magnetic profile to be varied, which has been very useful since we have tested several configurations, each requiring its own special magnetic profile for stability. The vacuum chamber uses Vacion pumps and produces a vacuum better than 10^{-6} Torr.

We have performed the first gain measurements of the slotted third-harmonic gyro-TWT amplifier to verify the amplifier's predicted stability. Single-section and two-section amplifiers were tested. The parameters of the two experiments are shown in Table IV. The one- and two-section amplifiers yielded small-signal gains of 13 dB and 25 dB, respectively, with bandwidths of 3% and 5% as shown in Figs. 25 and 26. The most important result of the tests was that they demonstrated stability from oscillation in the operating π mode. The measured threshold conditions for absolute instability are shown in Fig. 27. However, the two-section device did oscillate at the fourth-harmonic in the $4\pi/3$ mode, but this is expected to disappear when the sever is improved. Furthermore, there was low-level emission present at harmonics of the accelerator driver, but this is merely an artifact of the bunched[23,24] nature of the electron beam. Although a 1 kW TWT was used as the input, we were unable to drive either device into saturation due to the low insertion loss of the input coupler. Fabrication of a redesigned coupler is currently underway.

2.5 Harmonic Gyroklystron Amplifiers

We have also investigated harmonic gyroklystron amplifiers. An advantage of the gyroklystron is that the threat of oscillation is not as serious as in a gyro-TWT. A disadvantage is that its bandwidth is not nearly as broad as the gyro-TWT's.

2.5.1 Smooth-Bore Third-Harmonic TE_{31} Gyroklystron

We have developed the design for a 95 GHz third-harmonic gyroklystron amplifier, which exceeds most of the specifications in a recent ARPA research solicitation. The 1991 solicitation was to develop a compact 95 GHz fast-wave amplifier which 1) could generate ≥ 2 kW average power, 2) with ≥ 20% efficiency, 3) ≥ 30 dB saturated gain, 4) ~5% bandwidth, and 5) without requiring a superconducting solenoid. To meet the low magnetic field requirements, each of the three groups awarded contracts have proposed[14,25,26] using harmonic gyro (or penio) interactions utilizing axis-encircling electron beams within magnetron-type slotted waveguide. However, a major disadvantage of the slotted waveguide approach is that a large fraction of the electron beam will collide with the inside wall since the electrons must circle close to the inner radius to interact strongly with the fields fringing from the slots and furthermore, the slotted circuit is not extremely robust.

We have investigated the possibility of using a much more robust smooth-wall circuit. We have studied[27] a third-harmonic TE_{31} gyroklystron amplifier driven by an axis-encircling electron beam. The interception of the beam by the interaction circuit is no longer an issue because the beam circles far from the walls. The results of our simulation runs using K.R. Chu's self-consistent code[28] have been very encouraging. Figure 28 shows that good gain and efficiency can be achieved for a 70 kV beam. By setting the axis-encircling electron beam to be in resonance with the TE_{311} mode at the third cyclotron harmonic frequency, the beam will not interact at the stronger, lower cyclotron harmonic frequencies, which allows stable operation of the amplifier. The parameters for the proposed device are listed in Table V. For a 70 kV, 5 A electron beam with $v_\perp/v_\| = 2$ and $\Delta v_\|/v_\| = 10\%$, the 95 GHz three-cavity gyroklystron is predicted to yield 70 kW

with 20% efficiency, 0.2% bandwidth and a saturated gain of 35 dB. The nonlinear gain characteristics are shown in Fig. 29. By using a linear gyrotron code, it was verified that this amplifier is not even slightly threatened by oscillation in competing modes. Notice that this 95 GHz amplifier requires a magnetic field of only 12.4 kG, which can conveniently be produced by a fairly lightweight room-bore copper magnet. Thus, the only specification in the original ARPA solicitation that the proposed smooth-bore third-harmonic gyroklystron does not presently meet is the bandwidth, but it should be pointed out that stagger tuning the cavities could increase the bandwidth significantly. Furthermore, one of the three groups (Litton) funded by the ARPA program is also developing a device with a similar bandwidth.

2.5.2 Slotted Sixth-Harmonic Gyroklystron

We have also investigated slotted high-harmonic gyroklystron amplifiers. In a slotted harmonic gyroklystron's interaction circuit, the slotted gyro-TWT's long continuous tube is replaced by several cavities connected by smooth-bore cutoff drift-tubes of radius equal to the inner radius of the magnetron cavities. The cross-section of the cavities would be nearly identical with that of the gyro-TWT tube. For wide bandwidth (~ 1%), the Q value of the cavities must be quite low (~100).

We developed a linear theory[29] of the harmonic slotted gyroklystron amplifier. The theory is a modification of our linear theory of the harmonic smooth-wall gyroklystron.[30] The theory provides the small-signal gain and although it does not include beam loading, it is useful for choosing a device's initial parameters. To determine the nonlinear characteristics, we modified a self-consistent smooth-wall gyroklystron simulation code,[28] which had been written by K.R. Chu to simulate high power gyroklystrons. The nonlinear code does indeed agree with the linear theory in the limit of low beam current and weak input power as shown in Fig. 30, which also includes the predictions from a second linear theory, which is self-consistent. For low values of beam current, the three theories agree, but as the current approaches the critical value for oscillation, the gain from both the linear and nonlinear self-consistent theories, which include beam-loading, strongly diverges from the non-selfconsistent linear theory as it approaches infinity.

A parameter study[29] was performed of a sixth-harmonic slotted gyroklystron. A 95 GHz, three-cavity, 70 kV, 10 A, sixth-harmonic, slotted gyroklystron (Table VI), whose beam has $v_\perp/v_\parallel = 2$ and $\Delta v_\parallel/v_\parallel = 8\%$, was found to be capable of generating 70 kW with 30 dB saturated gain and 10% efficiency. The predicted transfer function is shown in Fig. 31.

3. References

1. A.T. Lin, K.R. Chu, C.C. Lin, C.S. Kou, D.B. McDermott, and N.C. Luhmann, Jr., "Marginal Stability Design Criterion for Gyro-TWT's and Comparison of Fundamental with Second Harmonic Operation," *Int. J. Electron.*, vol. 72, pp. 873-885, 1992.

2. Y.Y. Lau, K.R. Chu, L.R. Barnett and V.L. Granatstein, "Gyrotron Travelling Wave Amplifiers: Analysis of Oscillations," in *Infrared and Millimeter Waves*, Vol. 5, p. 267 (Academic Press, 1984, Ed. K. Button).

3. S.Y. Park, V.L. Granatstein, and R.K. Parker, "A Linear Theory and Design Study for a Gyrotron Backward Wave Oscillator." *Int. J. Electron.*, vol. 57, pp. 1109-1123, 1984.

4. A.K. Ganguly and S. Ahn, "Self-Consistent Large Signal Theory of a Gyrotron Traveling Wave Ampliier," *Int. J. Electron.*, vol. 53, p. 505, 1982.

5. D.S. Furuno, D.B. McDermott, C.S. Kou, N.C. Luhmann, Jr., and P. Vitello, "Theoretical and Experimental Investigation of a High-Harmonic Gyro-Travelling Wave Tube Amplifier," *Phys. Rev. Lett.* **62**, 1314 (1989).

6. C.S. Kou, Q.S. Wang, D.B. McDermott, A.T. Lin, K.R. Chu, and N.C. Luhmann, Jr., "High-Power Harmonic Gyro-TWT's--Part I: Linear Theory and Oscillation Study", *IEEE Trans.on Plasma Science*, vol. 20, no. 3, pp. 155-162, 1992.

7. Q.S. Wang, C.S. Kou, D.B. McDermott, A.T. Lin, K.R. Chu, and N.C. Luhmann, Jr., "High-Power Harmonic Gyro-TWT's--Part II: Nonlinear Thory and Design", *IEEE Trans.on Plasma Science*, vol. 20, no. 3, pp. 163-169, 1992.

8. Q.S. Wang, D.B. McDermott, A.T. Lin, N.C. Luhmann, Jr., and J. Pretterebner, "Single Stage High Power Second Harmonic Gyro-TWT," *Technical Digest of Int. Conf. on IR and Millimeter Waves*, p. 394, (1992).

9. Q.S. Wang, C.S. Kou, D.B. McDermott, A.J. Balkcum, K.R. Chu, and N.C. Luhmann, Jr., "Design of 1 MW, 140 GHz Third-Harmonic TE_{31} Gyro-TWT Amplifier," to be published, *IEEE Trans. on Plasma Science*'s Special Issue on High Power Microwave Generation, 22, October, 1994.

10 Y.Y. Lau and L.R. Barnett, "Theory of a Low Magnetic Field Gyrotron (Gyromagnetron)," *Int. J. Infrared and Millimeter Waves*, vol. 3, no. 5, pp. 619-643, 1982.

11. K.R. Chu and D. Dialetis, "Kinetic Theory of Harmonic Gyrotron Oscillation with Slotted Resonant Structure," in Infrared and Millimeter Waves, vol. 13, New York Academic Press, 1985, pp. 45-75.

12. A.K Ganguly, S. Ahn, and S.Y. Park, "Three Dimensional Theory of the Gyropeniotron Amplifier," *Int. J. Electron.*, vol. 65, no. 3, pp. 597-618, 1988.

13. C.K. Chong, D.B. McDermott, A.T. Balkcum, N.C. Luhmann, Jr., "Nonlinear Analysis of High-Harmonic Slotted Gyro-TWT Amplifier," *IEEE Trans. on Plasma Science*, vol. 20, no. 3, pp. 176-87, 1992.

14. W. DeHope, G. Hu, M. Mizuhara, J. Neilson, R. Schumacher, C. Chong, A. Lin, N. Luhmann, Jr., D. McDermott, and T. Stewart, "Design and Development of a Third-Harmonic, 95 GHz Gyro-TWT," in *Tech. Dig. of IEEE Int. Electron Dev. Meet. (IEDM)*, pp. 203-6, 1992.

15. W. DeHope, K. Felch, G. Hu, M. Mizuhara, J. Neilson, P. Reysner, R. Schumacher, B. Stockwell, A. Balkcum, C. Chong, N. Luhmann, Jr., and D. McDermott, "Initial Tests of a High Power, Broadband Gyro-TWT," *Technical Digest of Int. Electron Devices Meeting*, p. 355, 1993.

16. 10. S.E. Miller, "Coupled Wave Theory and Waveguide Applications," *Bell System Tech. Journal*, 661 (May 1954)

17. M. Thumm, "High-Power Millimeter-Wave Mode Converters in Overmoded Circular Waveguides Using Periodic Wall Perturbations," *Int. J. Electronics* 57, 1225 (1984).

18. N.R. Vanderplaats, H.E. Brown, and S. Ahn, "Magnetically Shielded Electron Guns with a Center Magnetic Post," *Tech. Digest of IEDM*, 336 (1981).

19. G.P. Scheitrum and R.B. True, "Triple Pole Piece Magnetic Field Reversal Element for Generation of High Rotational Energy Beams," *Tech. Digest of IEDM*, 332 (1981).

20. G.P. Scheitrum, R.S. Symons, and R.B. True, "Low Velocity Spread Axis Encircling Electron Beam Forming System," *Tech. Digest of IEDM*, 743 (1989).

21. D.B. McDermott, D.S. Furuno, and N.C. Luhmann, Jr., "Production of Relativistic, Rotating Electron Beams by Gyroresonant RF Acceleration in a TE111 Cavity," *J. Appl. Physics*, vol. 58, no. 12, pp. 4501-8, 1985.

22. H.R. Jory and A.W. Trivelpiece, "Charged Particle Motion in Large-Amplitude Electromagnetic Fields," *J. Appl. Phys.* **39**, 3053 (1968).

23. C.S. Kou, D.B. McDermott, N.C. Luhmann, Jr., and K.R. Chu, "Prebunched High-Harmonic Gyrotron," *IEEE Trans. Plasma Science* **18**, 343 (1990).

24. A.J. Balkcum, D.B. McDermott, F.V. Hartemann, and N.C. Luhmann, Jr., "High-Harmonic Gyrofrequency Multiplier," to be published, *IEEE Trans. on Plasma Science*'s Special Issue on High Power Microwave Generation, 22, October, 1994.

25. T.A. Hargreaves, G.P. Scheitrum, T. Bemis and L. Higgins, in *Tech. Dig. of IEEE Int. Electron Device Meeting (IEDM)*, 347 (1993).

26. G. Dohler, D. Gallagher, J. Richards, and F. Scafuri, in *Tech. Dig. of IEEE Int. Electron Device Meeting (IEDM)*, 363 (1993).

27. J.D. McNally, D.B. McDermott, Q.S. Wang, F.V. Hartemann, and N.C. Luhmann, Jr., "High Performance, 70 kV Third-Harmonic Smooth-Bore Gyroklystron Amplifier," to be published, *IEEE Trans. on Plasma Science*'s Special Issue on High Power Microwave Generation, 22, October, 1994.

28. K.R. Chu, V.L. Granatstein, P.E. Latham, W. Lawson, and C.D. Striffler, "A 30 MW Gyroklystron-Amplifier Design for High-Energy Linear Accelerators," IEEE Trans. Plasma Sci., vol. PS-13, pp. 424-34, 1985.

29. D.B. McDermott, C.K. Chong, N.C. Luhmann, Jr., K.R. Chu, and D. Dialetis, "High Harmonic Slotted Gyroklystron Amplifier: Linear Theory and Nonlinear Simulation," to be published, *IEEE Trans. on Plasma Science*'s Special Issue on High Power Microwave Generation, 22, October, 1994.

30. D.S. Furuno, D.B. McDermott, N.C. Luhmann, Jr., and P. Vitello, "A High-Harmonic Gyro-Klystron Amplifier: Theory and Experiment," *Int. J. Electronics*, vol. 57, 1151 (1984).

4. Figures and Tables

Table I. Operating parameters for 16 GHz single-section second-harmonic gyro-TWT proof-of-principle experiment.

Beam Voltage	80 kV
Beam Current	20 A
α (=$v_\perp/v_\parallel$)	1.0
Magnetic Field	2.9 kG
Cyclotron Harmonic	2^{nd}
Mode	TE_{21}
Wall Radius, r_w	0.95 cm
r_{gc}/r_w	0.4
$\Delta v_\parallel/v_\parallel$	12%
B/B_g	0.96
Circuit Length	65 cm

Table II. Design parameters for 140 GHz third-harmonic TE_{31} gyro-TWT amplifier with (a) axis-encircling and (b) MIG beams.

	(a) Cusp Beam	(b) MIG Beam
Beam Voltage	100 kV	100 kV
Beam Current	50 A	50 A
α (=$v_\perp/v_\parallel$)	1.0	1.0
Magnetic Field	17 kG	17 kG
Cyclotron Harmonic	3^{rd}	3^{rd}
Mode	TE_{31}	TE_{31}
Wall Radius, r_w	0.15 cm	0.15 cm
r_{gc}/r_w	0.0	0. 3
$\Delta v_\parallel/v_\parallel$	5%	5%
B/B_g	0.99	0.99
Section Length	3 cm (two)	10 cm
Sever Length	0.75 cm	none
Circuit Length	6.75 cm	10 cm

Table III. Design parameters of three-section, 95 GHz slotted third-harmonic gyro-TWT amplifier.

Beam Voltage	50 kV
Beam Current	3 A
α (=$v_\perp/v_\parallel$)	1.4
Magnetic Field	11 kG
Cyclotron Harmonic	3^{rd}
Mode	π mode
Number of Vanes	6
Inner Circuit Radius, *a*	0.107 cm
Outer Circuit Radius, *b*	0.147 cm
r_L/a	0.53
r_c/a	0.0
$\Delta r_{gc}/a$	10%
$\Delta v_\parallel/v_\parallel$	8%
B/B_g	0.99
Section Length	3.0 cm:3.0 cm:4.0 cm
Circuit Length	11.6 cm

Table IV. Operating parameters for single-section and two-section third-harmonic slotted gyro-TWT amplifier proof-of-principle experiments.

	(a) 1-Section	(b) 2-Section
Beam Voltage	62 kV	75 kV
Beam Current	2.4 A	2.6 A
Magnetic Field	1.3 kG	1.3 kG
Cyclotron Harmonic	3rd	3rd
Number of Vanes	6	6
α ($v_\perp/v_\parallel$)	1.0	1.4
r_c/r_w	0.0	0.0
$\Delta v_\parallel/v_\parallel$	≤5%	≤5%
$\Delta r_c/a$	22%	22%
Electron Larmor Radius, r_L	0.47 cm	0.60 cm
Inner Circuit Radius, *a*	0.96 cm	0.96 cm
Outer Circuit Radius, *b*	1.37 cm	1.37 cm
Section Length	37.1 cm	30.5 cm
Sever Length	none	8.35 cm
Circuit Length	37.1 cm	69.35 cm

Table V. Design parameters for 95 GHz, three-cavity third-harmonic TE_{311} smooth-bore gyroklystron amplifier.

Beam Voltage	70 kV
Beam Current	5 A
α ($=v_\perp/v_\parallel$)	2.0
Magnetic Field	12.4 kG
Cyclotron harmonic	3rd
Mode	TE_{311}
Cavity Radii, r_w	0.21 cm
Cavity Length	1.26 cm
Cavity Q's	225
Drift-Tube Length	1.89 cm
r_c/r_w	0.0
$\Delta v_\parallel/v_\parallel$	10%
$\Delta r_{gc}/r_w$	10%
Circuit Length	5.04 cm

Table VI. Parameters parameters for 70 kW, 95 GHz, sixth-harmonic slotted gyroklystron.

Beam Voltage	70 kV
Beam Current	10 A
α ($=v_\perp/v_\parallel$)	2.0
Magnetic Field	6.2 kG
Cyclotron Harmonic	6th
Number of Vanes	12
Inner Circuit Radius, *a*	0.078 cm
Outer Circuit Radius, *b*	0.102 cm
Cavity Length	1.26 cm
Cavity Q's	185
Drift-Tube Length	2.52 cm
r_L/a	0.8
r_c/a	0.0
$\Delta v_\parallel/v_\parallel$	8%
$\Delta r_{gc}/a$	10%
Circuit Length	6.30 cm

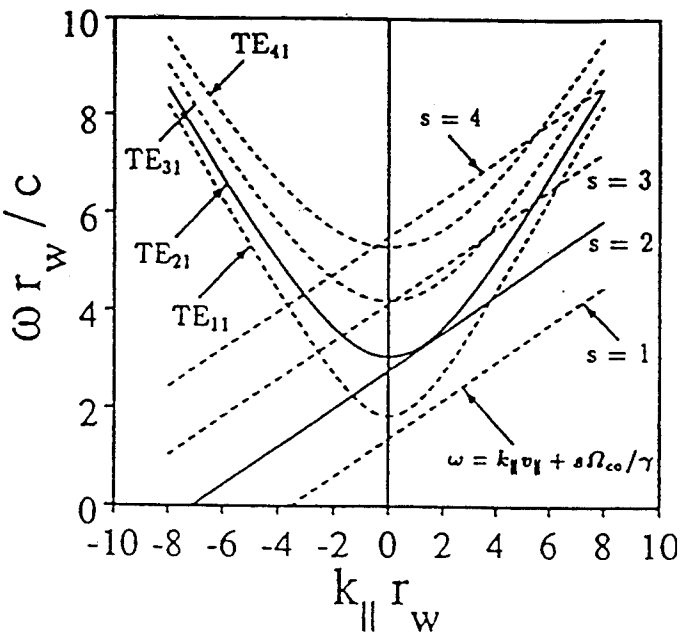

Fig. 1 Uncoupled dispersion relation of operating mode (intersection of unbroken curves) and likely oscillating modes (intersections of broken curves with negative $k_{||}$) for second harmonic TE_{21} gyro-TWT amplifier.

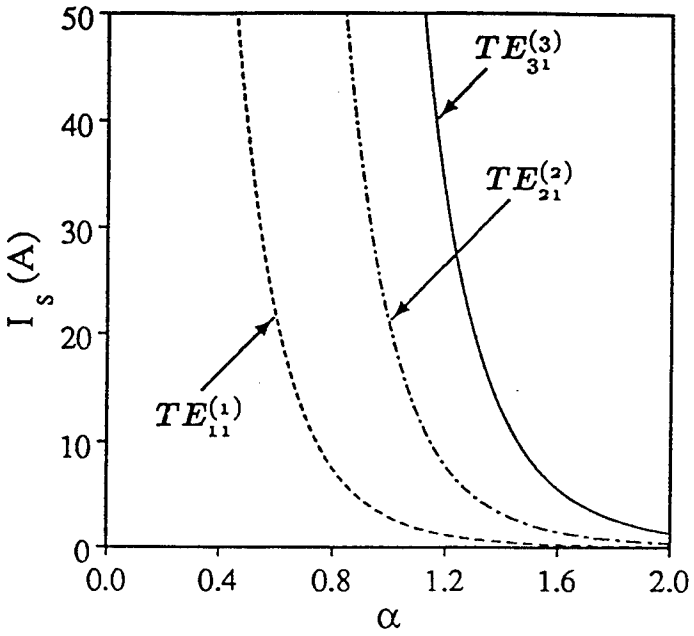

Fig. 2 Dependence on velocity ratio α of threshold beam current from analytical theory for absolute instability in s^{th}-harmonic TE_{s1} gyro-TWT with 100 kV axis-encircling beam for s = 1, 2 and 3.

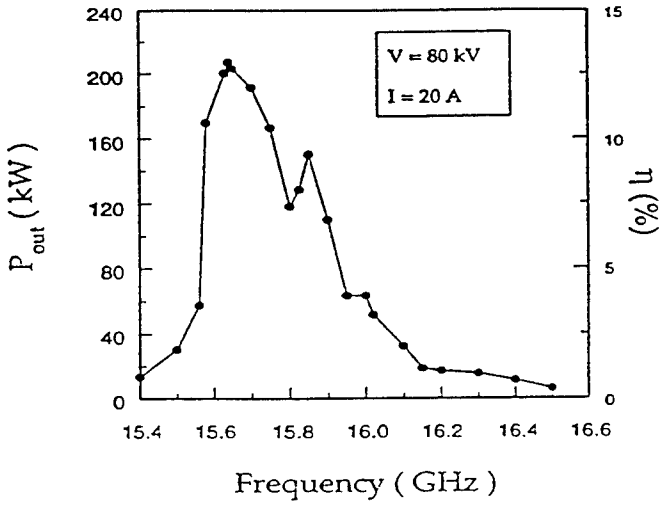

Fig. 3 Measured dependence of output power on frequency in the second-harmonic TE_{21} gyro-TWT (Table I).

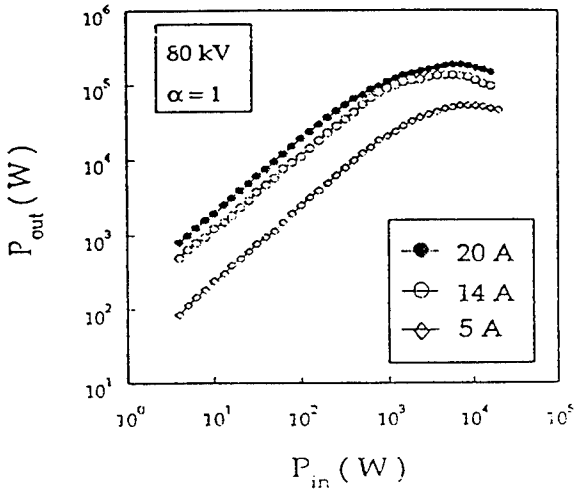

Fig. 4 Dependence of output power on rf input power in the second-harmonic TE_{21} gyro-TWT (Table I).

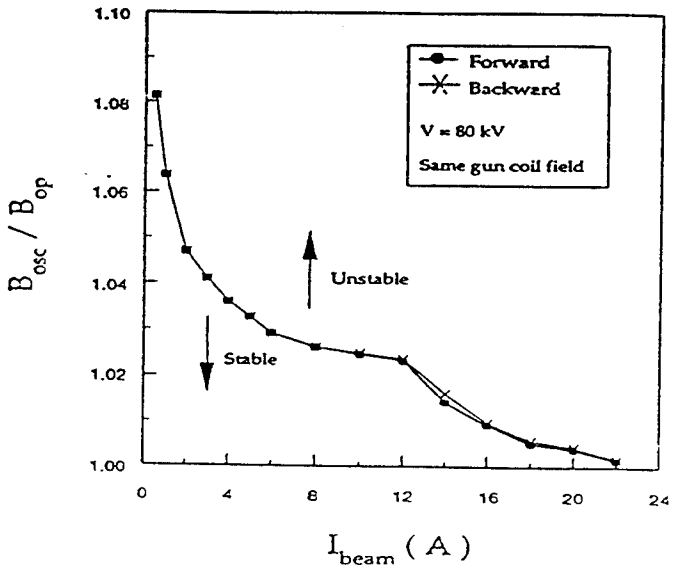

Fig. 5 Measured dependence of the start-oscillation magnetic field normalized to the operating magnetic field in the second-harmonic TE_{21} gyro-TWT (Table I).

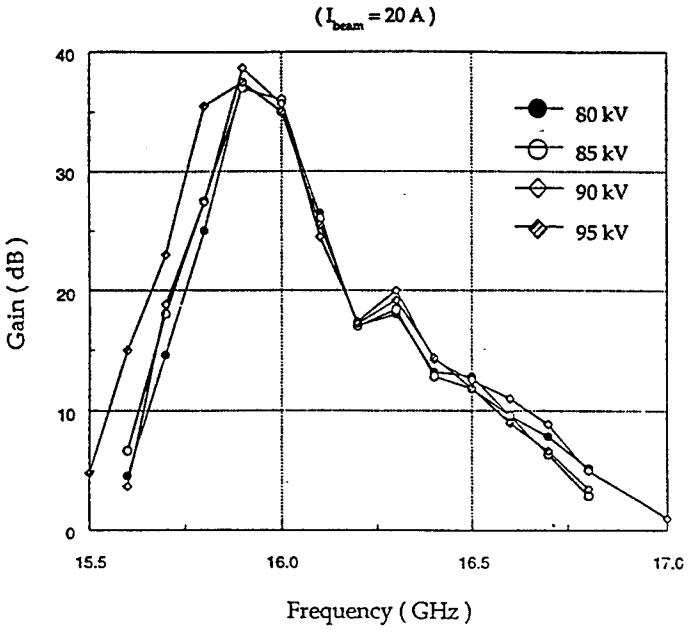

Fig. 6 Measured dependence of small-signal gain on frequency in the second-harmonic TE_{21} gyro-TWT.

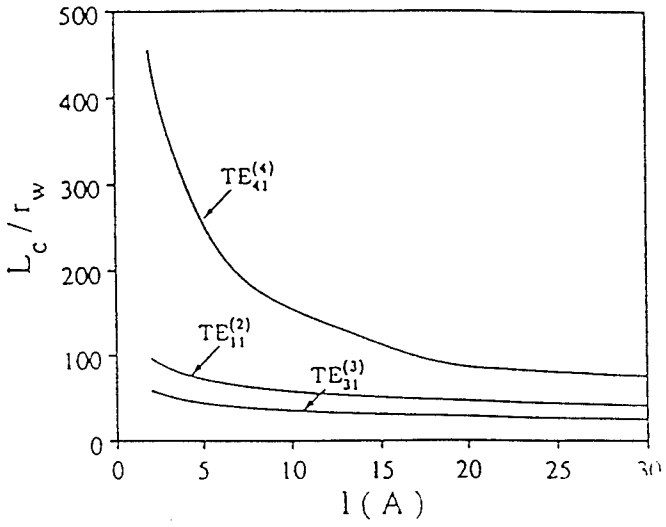

Fig. 7 Dependence of critical oscillation length for $TE_{31}^{(3)}$, $TE_{11}^{(2)}$ and $TE_{41}^{(4)}$ gyro-BWO modes in second-harmonic TE_{21} gyro-TWT (100 kV, $v_\perp/v_\parallel = 1$, $r_c/r_w = 0.4$, r_w is the wall radius).

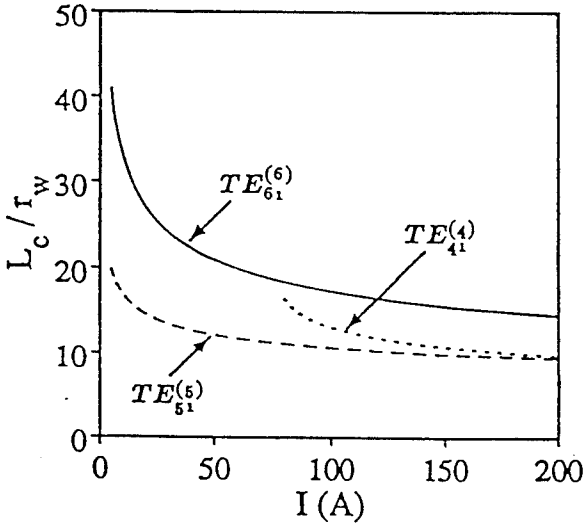

Fig. 8 Dependence on beam current of critical oscillation length from analytical theory for dominant gyro-BWO modes in third-harmonic TE_{31} gyro-TWT (100 kV, $\alpha = v_\perp/v_\parallel = 1$, $r_c = 0$).

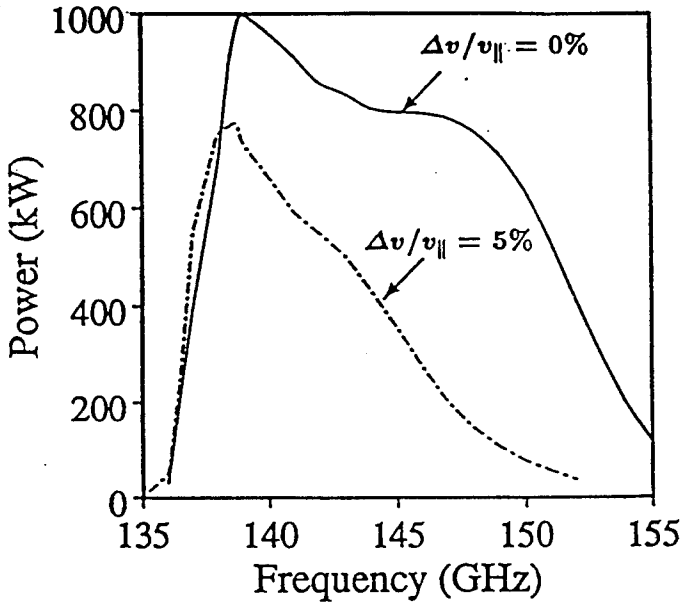

Fig. 9 Predicted constant-drive bandwidth of third-harmonic TE_{31} gyro-TWT (Table II(a)).

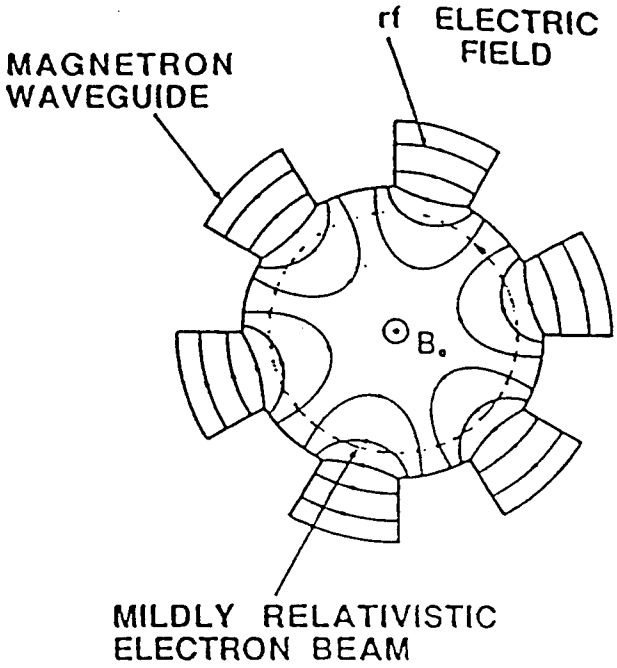

Fig. 10 Cross-sectional view of slotted gyro-TWT with six vanes and showing the rf electric field pattern of the π mode.

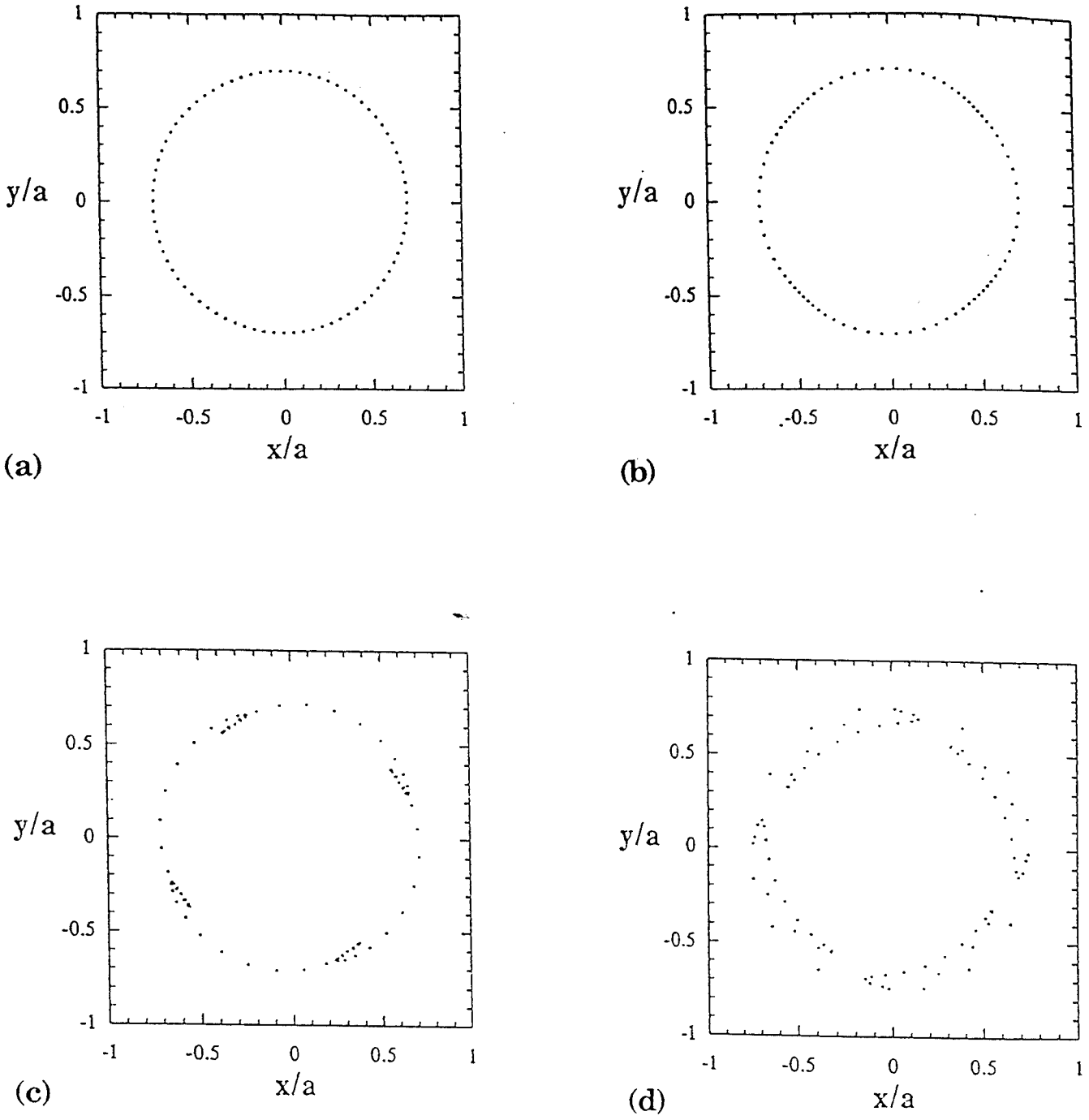

Fig. 11 Cross-sectional distribution of (a) initial electron beam and beam during (b) early, (c) middle and (d) late linear amplification stages of fourth-harmonic gyro-TWT interaction.

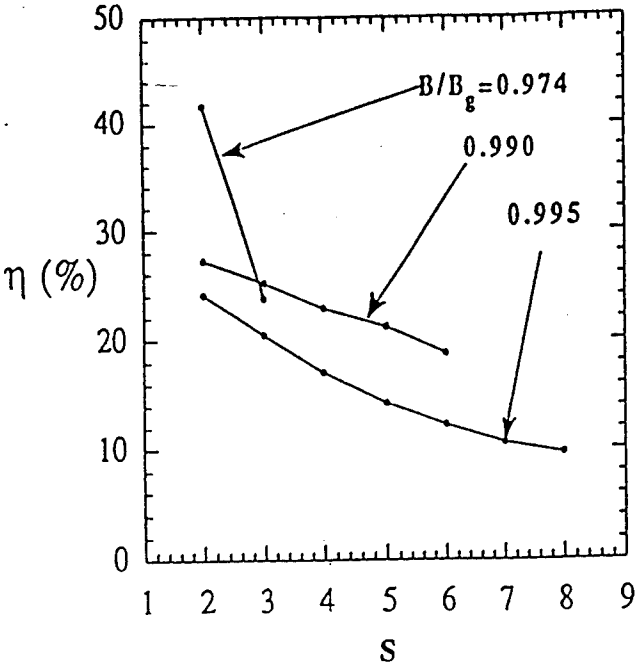

Fig. 12 Dependence of slotted gyro-TWT's saturation efficiency on harmonic number for several values of magnetic tuning ratio (π mode, 60 kV, 5 A, $v_\perp/v_{||}$=1.5, r_L/a=0.7, $\omega/\omega_c=\gamma_{||}$, $\Delta v_{||}$=0, and Δr_c=0).

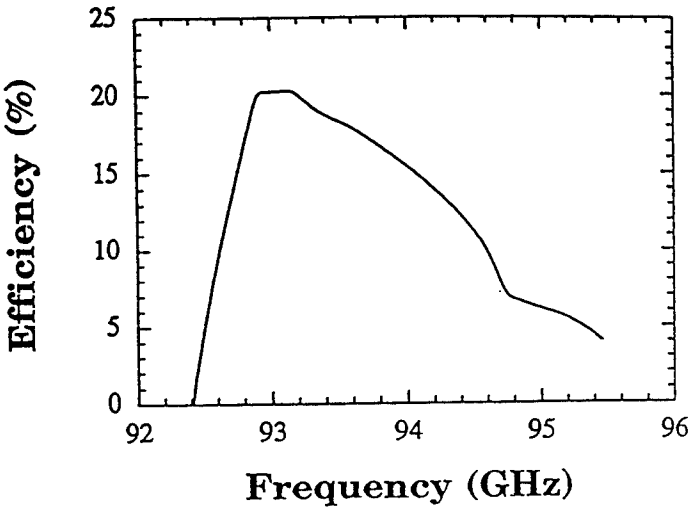

Fig. 13 Predicted constant-drive bandwidth of third-harmonic slotted gyro-TWT (Table III).

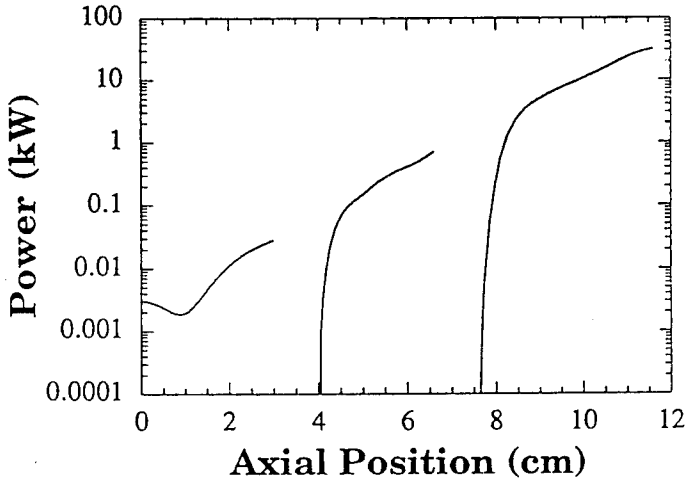

Fig. 14 Predicted spatial growth of 94 GHz power in third-harmonic slotted gyro-TWT (Table III).

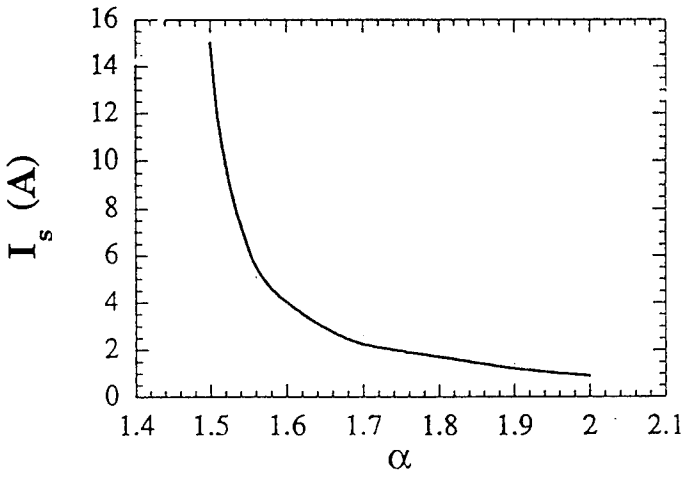

Fig. 15 Predicted dependence on $v_\perp/v_{||}$ of the threshold beam current for absolute instability of the π mode in the third-harmonic slotted gyro-TWT (Table III).

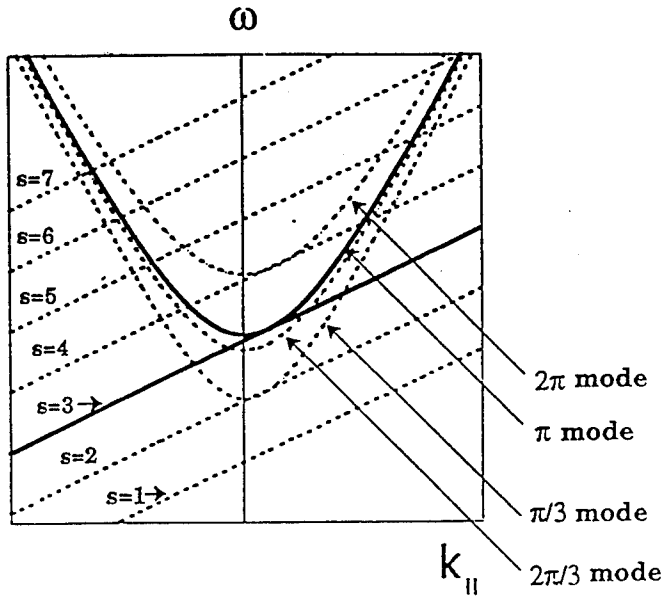

Fig. 16 Uncoupled dispersion diagram of slotted third-harmonic gyro-TWT (Table III).

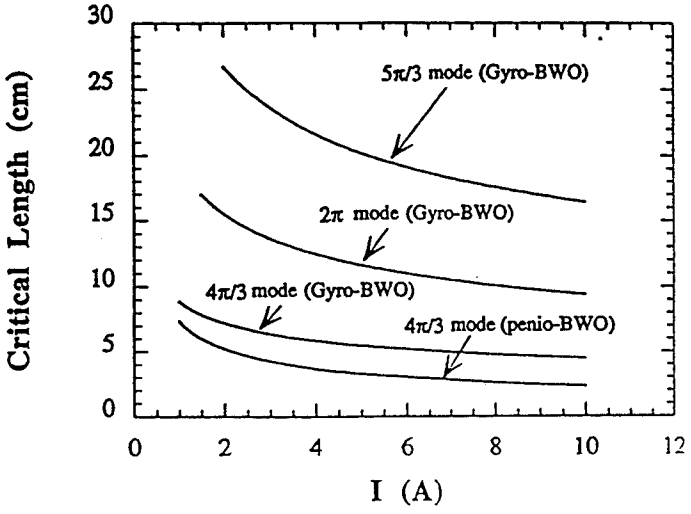

Fig. 17 Dependence on the beam's current of the critical oscillation length for the dominant penio-BWO and gyro-BWO modes in the slotted third-harmonic gyro-TWT (Table III).

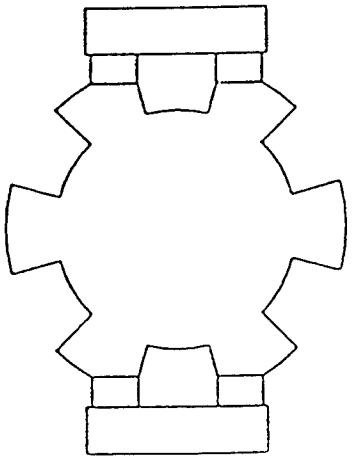

Fig. 18 Schematic of dual-feed, 0 dB slotted directional input coupler.

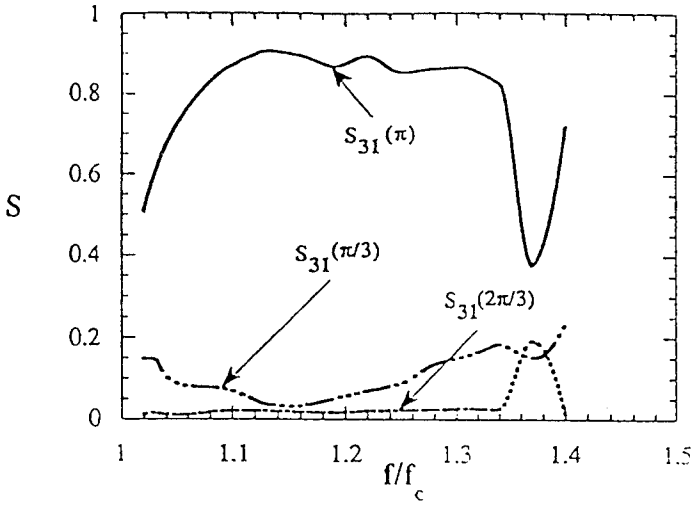

Fig. 19 Dependence of S_{31} on frequency for desired π mode and spurious π/3 and 2π/3 modes in slotted input coupler as predicted by HFSS.

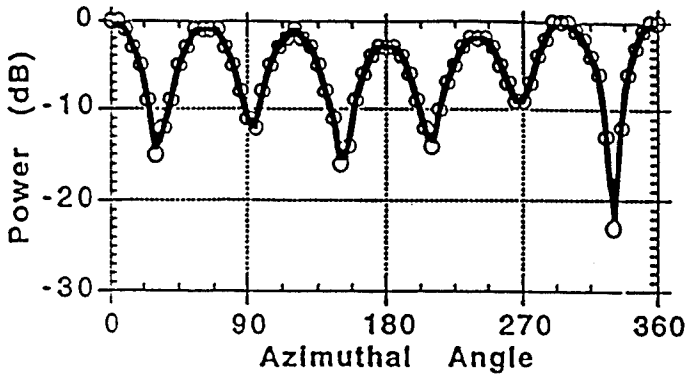

Fig. 20 Measured field pattern of wave launched by slotted input coupler.

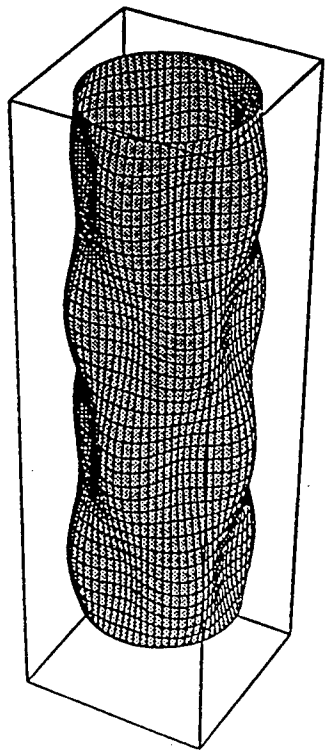

Fig. 21 Schematic of a two-period TE_{31}/TE_{11} mode converter.

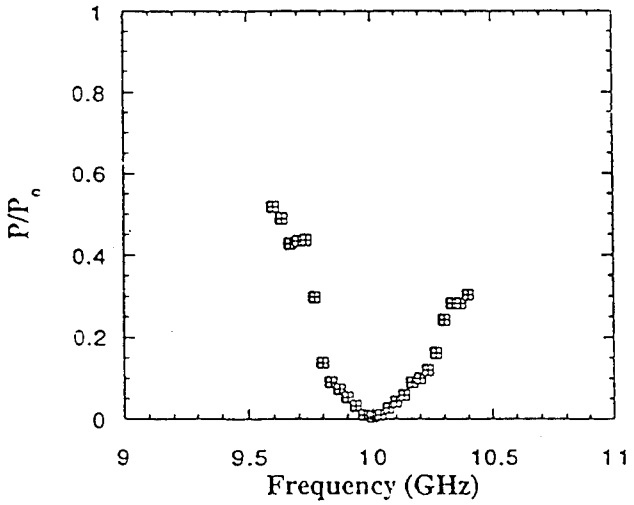

Fig. 22 Measured bandwidth for four-period m=4 beat-wave mode converter of power remaining in the TE_{11} input wave.

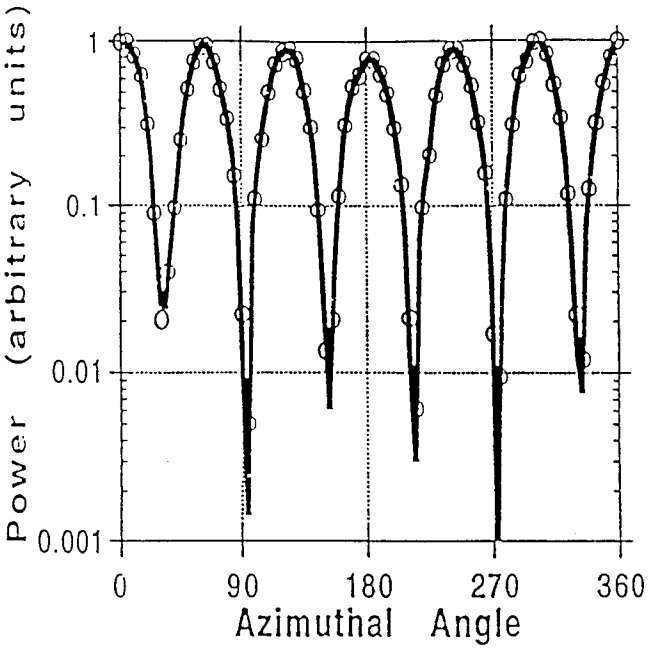

Fig. 23 Measured field pattern of wave transformed by four-period m=4 beat-wave mode converter (TE_{11} input wave).

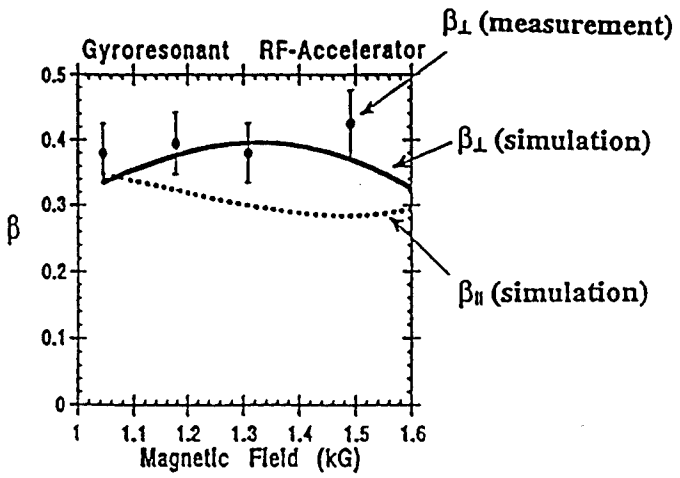

Fig. 24 Dependence on magnetic field of measured transverse velocity and axial and transverse velocities from simulation in TE_{111} gyroresonant rf accelerator.

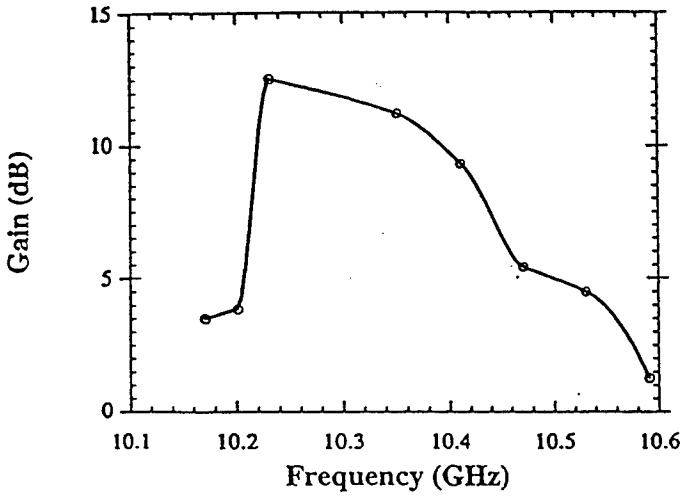

Fig. 25 Unsaturated constant-drive bandwidth of one-section third-harmonic slotted gyro-TWT amplifier (Table IV(a)).

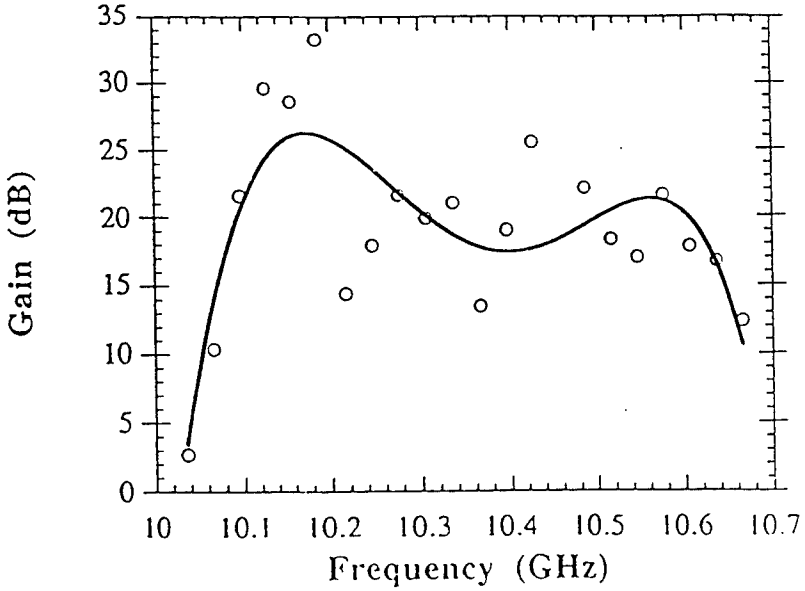

Fig. 26 Unsaturated constant-drive bandwidth of two-section third-harmonic slotted gyro-TWT amplifier (Table IV(b)).

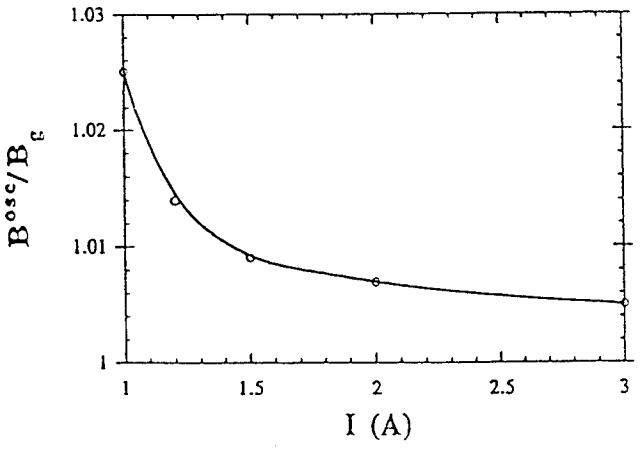

Fig. 27 Measured dependence on beam current of magnetic field normalized to the operating magnetic field for the onset of the absolute instability in two-section third-harmonic slotted gyro-TWT amplifier (Table IV(b)).

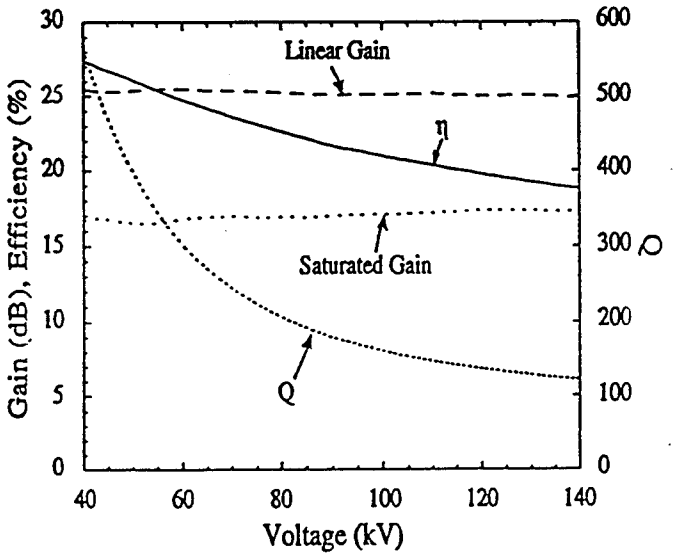

Fig. 28 Dependence of linear gain, saturated gain, efficiency, and Q on beam voltage for two-cavity third-harmonic smooth-bore gyroklystron with parameters otherwise given by Table V.

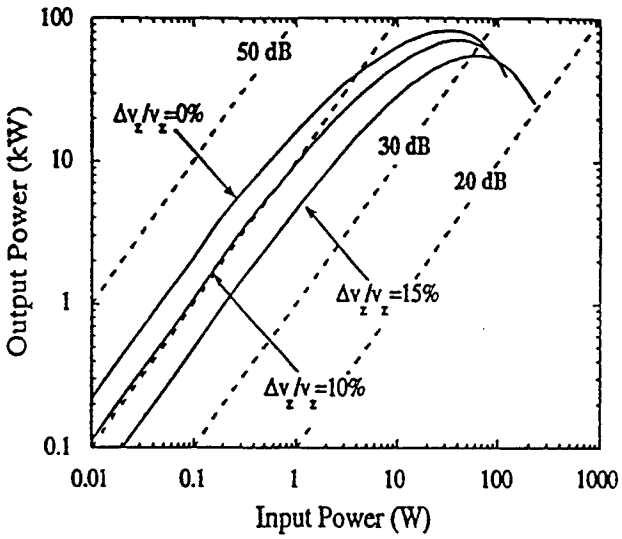

Fig. 29 Dependence of output power on input power for 70 kV, three-cavity third-harmonic smooth-bore gyroklystron (Table V).

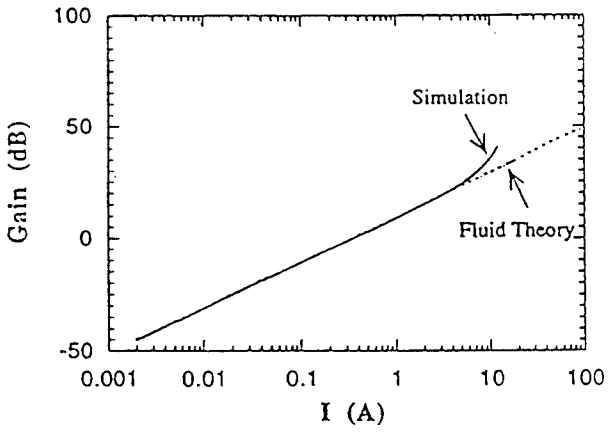

Fig. 30. Dependence of small-signal gain on electron beam current in two-cavity, sixth-harmonic slotted gyro-klystron as predicted by fluid theory and linear and nonlinear simulation codes (Table VI with $L_d = 14\lambda$ and ideal beam). The two curves from simulation are identical.

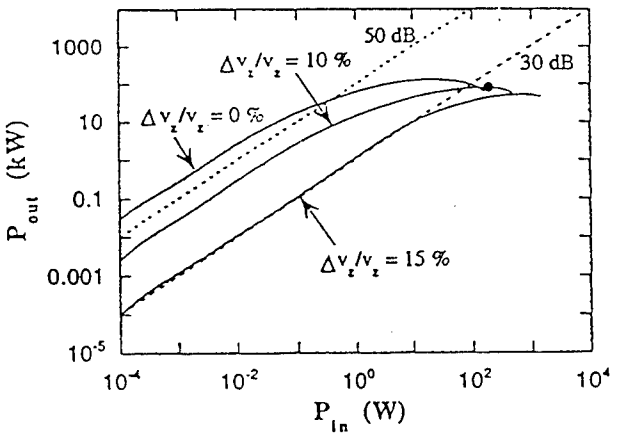

Fig. 31. Dependence of output power on input power in 70 kV, 95 GHz, three-cavity, slotted third-harmonic gyro-klystron amplifier (Table VI) for four values of axial velocity spread ($\Delta v_{\|}/v_{\|}$ = 0%, 5%, 10% and 15%).

5. Publications and Conference Presentations during 10/1/91--9/30/94

C.K. Chong, D.B. McDermott, A.J. Balkcum, and N.C. Luhmann, Jr., "Nonlinear Analysis of High-Harmonic Slotted Gyro-TWT Amplifier," *IEEE Trans. on Plasma Science*, 20, 176 (1992).

C.S. Kou, Q.S. Wang, D.B. McDermott, A.T. Lin, K.R. Chu, and N.C. Luhmann, Jr., "High Power Harmonic Gyro-TWTs - Part I: Linear Theory and Oscillation Study," *IEEE Trans on Plasma Science*, 20, 155 (1992).

Q.S. Wang, D.B. McDermott, C.S. Kou, A.T. Lin, K.R. Chu, and N.C. Luhmann, Jr., "High-Power Harmonic Gyro-TWT's - Part II: Nonlinear Theory and Design," *IEEE Trans. on Plasma Science*, 20, 163 (1992).

Q.S. Wang, D.B. McDermott, A.T. Lin, N.C. Luhmann, Jr., and J. Pretterebner, "35 GHz High Power, Second Harmonic Gyro-TWT Amplifier," *Technical Digest of Int. Electron Devices Meeting*, p. 207, (1992).

Q.S. Wang, C.S. Kou, D.B. McDermott, F.V. Hartemann, A.J. Balkcum, K.R. Chu, and N.C. Luhmann, Jr., "Design of 1 MW, 140 GHz Third-Harmonic TE_{31} Gyro-TWT Amplifier," to be published, *IEEE Trans. on Plasma Science*'s Special Issue on High Power Microwave Generation, 22, October, 1994.

D.B. McDermott, C.K. Chong, N.C. Luhmann, Jr., K.R. Chu, and D. Dialetis, "High Harmonic Slotted Gyroklystron Amplifier: Linear Theory and Nonlinear Simulation," to be published, *IEEE Trans. on Plasma Science*'s Special Issue on High Power Microwave Generation, 22, October, 1994.

J.D. McNally, D.B. McDermott, Q.S. Wang, F.V. Hartemann, and N.C. Luhmann, Jr., "High Performance, 70 kV Third-Harmonic Smooth-Bore Gyroklystron Amplifier," to be published, *IEEE Trans. on Plasma Science*'s Special Issue on High Power Microwave Generation, 22, October, 1994.

Q.S. Wang, C.K. Chong, C.S. Kou, D.B. McDermott, N.C. Luhmann, Jr., A.T. Lin, and K.R. Chu, "High Power, Harmonic Gyro-TWTs," *Technical Digest of 16th Int. Conf. on Infrared and Millimeter Waves*, Lausanne, Switzerland, 1991.

C.K. Chong, D.B. McDermott, and N.C. Luhmann, Jr., "40 kW Fourth-Harmonic Gyromagnetron-TWT," *Bull. Am. Phys. Soc.*, 36, 2404, (1991).

Q.S. Wang, C.K. Chong, C.S. Kou, D.B. McDermott, N.C. Luhmann, Jr., A.T. Lin, and K.R. Chu, "High Power, Second Harmonic Gyro-TWT," *Bull. Am. Phys. Soc.*, 36, 2405, (1991).

Q.S. Wang, C.K. Chong, C.S. Kou, D.B. McDermott, A.T. Lin, K.R. Chu, and N.C. Luhmann, Jr., "High-Power, Harmonic Gyro-TWT Design," *Proceedings of SPIE Conf. on Intense Microwave and Particle Beams*, Los Angeles, California, 1992.

K.C. Leou, T.R. Stephenson, J.D. McNally, G. Vasilakos, G.D. Ramlow, M.P. Bobys, D.B. McDermott, and N.C. Luhmann, Jr., "Fast-Wave Research at UCLA: Gyro-TWT, Gyro-BWO and Gyro-Klystron," *Digest of Microwave Power Tube Conference*, Monterey, California, 1992.

C.K. Chong, Q.S. Wang, C.S. Kou, T.L. Stewart, A.J. Balkcum, C.F. Kinney, D.B. McDermott, A.T. Lin, K.R. Chu, and N.C. Luhmann, Jr., "Harmonic 35 GHz Gyro-TWT Amplifiers at UCLA," *Digest of Microwave Power Tube Conference*, Monterey, California, 1992.

Q.S. Wang, D.B. McDermott, N.C. Luhmann, Jr., A.T. Lin, C.S. Kou, and K.R. Chu, "Harmonic Gyro-TWT Amplifier for High Power," *Technical Digest of 9th Intl. Conf. on High Power Particle Beams*, Washington, D.C., 1992.

Q.S. Wang, D.B. McDermott, A.T. Lin, N.C. Luhmann, Jr., and J. Pretterebner, "High Power Harmonic Gyro-TWT," *Bull. Am. Phys. Soc.*, 37, 1538, (1992).

C.K. Chong, D.B. McDermott, T.L. Stewart, C.F. Kinney, A.J. Balkcum, N.C. Luhmann, Jr., A.T. Lin, W.J. DeHope, and J. Pretterebner, " Design of 95 GHz Third-Harmonic Two-Section Gyro-TWT Amplifier," *Bull. Am. Phys. Soc.*, 37, 1538, (1992).

Q.S. Wang, D.B. McDermott, A.T. Lin, N.C. Luhmann, Jr., and J. Pretterebner, "Single Stage High Power Second Harmonic Gyro-TWT," *Technical Digest of Int. Conf. on IR and Millimeter Waves*, P. 394, (1992).

C.K. Chong, D.B. McDermott, T.L. Stewart, C.F. Kinney, A.J. Balkcum, A.T. Lin, N.C. Luhmann, Jr., J. Pretterebner, and W.J. DeHope, "Design of a 95 GHz Slotted Third-Harmonic Gyro-TWT Amplifier," *Technical Digest of Int. Conf. on IR and Millimeter Waves*, P. 388, (1992).

D.B. McDermott, C.K. Chong, and N.C. Luhmann, Jr., " 35 GHz Slotted Fourth-Harmonic Gyro-Klystron," *Technical Digest of Int. Conf. on IR and Millimeter Waves*, P. 252, (1992).

C.K. Chong, D.B. McDermott, T.L. Stewart, A.J. Balkcum, C.F. Kinney, A.T. Lin, N.C. Luhmann, Jr., and J. Pretterebner, "95 GHz Third-Harmonic Slotted Gyro-TWT Amplifier," *Proceedings of SPIE Conf. on Intense Microwave Pulses*, 1993.

Q.S. Wang, D.B. McDermott, A.T. Lin, N.C. Luhmann, Jr., and J. Pretterebner, "Development of High-Power Second Harmonic Gyro-TWT," *Proceedings of SPIE Conf. on Intense Microwave Pulses*, 1993.

K.C. Leou, Q.S. Wang, C.K. Chong, A.J. Balkcum, S.N. Fochs, E. Garland, J. Pretterebner, A.T. Lin, D.B. McDermott, F. Hartemann, and N.C. Luhmann, Jr., "Gyro-TWT Amplifiers at UCLA," *Digest of Int. Conf. on IR and Millimeter Waves*, 1993.

C.K. Chong, Q.S. Wang, K.C. Leou, J.D. McNally, M.P. Bobys, A.J. Balkcum, D.B. McDermott, F. Hartemann, J. Pretterebner, A.T. Lin, and N.C. Luhmann, Jr., "High-Harmonic Gyro-Amplifiers," submitted to *Proceedings of Second Annual Vacuum Electronic Conf.*, 1993.

J.D. McNally, M.P. Bobys, F.V. Hartemann, D.B. McDermott, and N.C. Luhmann, Jr., "Gyroklystron Amplifiers at UCLA," *Proceedings of Asia-Pacific Conference*, vol. 1, p. 6-74, 1993.

K.C. Leou, Q.S. Wang, C.K. Chong, A.J. Balkcum, J. Pretterebner, A.T. Lin, D.B. McDermott, F. Hartemann, and N.C. Luhmann, Jr., "Recent UCLA Fast-Wave "Amplifier Developments," *Proceedings of Asia-Pacific Conference*, vol. 1, p. 6-66, 1993.

J.D. McNally, M.P. Bobys, D.B. McDermott, F.V. Hartemann, and N.C. Luhmann, Jr., "Smooth-Bore Third-Harmonic TE_{311} Gyro-Klystron," *Bull. Am. Phys. Soc.* 38, 2001 (1993).

Q.S. Wang, D.B. McDermott, F.V. Hartemann, E.S. Garland, and N.C. Luhmann, Jr., "High Power, Second Harmonic TE_{21} Gyro-TWT," *Bull. Am. Phys. Soc.* 38, 2000 (1993).

D.B. McDermott, C.K. Chong, F.V. Hartemann, N.C. Luhmann, Jr., and A.T. Lin, " Slotted Third-Harmonic Peniotron Forward-Wave Oscillator," *Bull. Am. Phys. Soc.* 38, 2001 (1993).

C.K. Chong, D.B. McDermott, F.V. Hartemann, A.J. Balkcum, N.C. Luhmann, Jr., and W.J. DeHope, "95 GHz Slotted Third-Harmonic Gyro-TWT," *Bull. Am. Phys. Soc.* 38, 2001 (1993).

A.T. Lin, C.K. Chong, D.B. McDermott, A.J. Balkcum, F.V. Hartemann, and N.C. Luhmann, Jr., "Slotted Third-Harmonic Peniotron Forward-Wave Oscillator," Proc. of *SPIE Conf. on High Power Microwaves*, Los Angeles, CA, 1994.

C.K. Chong, D.B. McDermott, A.J. Balkcum, F.V. Hartemann, N.C. Luhmann, Jr., and W.J. DeHope, "Scaled Tests of Varian's 95 GHz Slotted Third-Harmonic Gyro-TWT," Proc. of *SPIE Conf. on High Power Microwaves*, Los Angeles, CA, 1994.

K.C. Leou, Q.S. Wang, D.B. McDermott, F.V. Hartemann, C.K. Chong, and N.C. Luhmann, Jr., "Recent Gyro-TWT Amplifier Developments at UCD," Digest of *Microwave Power Tube Conference*, 3B.5, Monterey, CA, 1994.

J.D. McNally, D.B. McDermott, F.V. Hartemann, and N.C. Luhmann, Jr., "Smooth-Bore Third-Harmonic TE_{311} Gyroklystron," Digest of *Microwave Power Tube Conference*, 2E.3, Monterey, CA, 1994.

C.K. Chong, D.B. McDermott, A.J. Balkcum, N.C. Luhmann, Jr., A.T. Lin, and W.J. DeHope, "Slotted Third-Harmonic Gyro-TWT Results," submitted to 36th Annual Meeting, APS Div. of Plasma Physics, Minneapolis, MN, 1994.

Q.S. Wang, D.B. McDermott, A.J. Balkcum and N.C. Luhmann, Jr., "High Power, n^{th}-Harmonic TE_{n1} Gyro-TWT's: 200 kW Second-Harmonic Results and 1 MW Third-Harmonic Design," submitted to 36th Annual Meeting, APS Div. of Plasma Physics, Minneapolis, MN, 1994.

K.C. Leou, Q.S. Wang, C.K. Chong, D.B. McDermott, A.J. Balkcum, F.V. Hartemann, and N.C. Luhmann, Jr., "Gyro-TWT Amplifier Development at UCD," submitted to 19^{th} Int. Conf. on Infrared and Milimeter Waves, Sendai, Japan, 1994.

A.T. Lin, C.K. Chong, D.B. McDermott, A.J. Balkcum, F.V. Hartemann, and N.C. Luhmann, Jr., "Third-Harmonic Slotted Forward-Wave Peniotron," submitted to 19^{th} Int. Conf. on Infrared and Milimeter Waves, Sendai, Japan, 1994.